*Article*

# The Peritectic Reaction of Olivine as the Mechanism of the Ultrabasic–Basic Evolution of the Diamond-Forming Silicate-Carbonate-(C-O-H) System: Experiments at 6.0 GPa

Yuriy A. Litvin *, Anastasiya V. Kuzyura and Anna V. Spivak [ID]

Korzhinskii Institute of Experimental Mineralogy, Center of Russian Academy of Sciences, 142432 Moscow, Russia; shu25@rambler.ru (A.V.K.); spivak@iem.ac.ru (A.V.S.)
* Correspondence: litvin@iem.ac.ru; Tel.: +7-4965225876

**Abstract:** Melting phase relations of the diamond-forming olivine (Ol)–jadeite (Jd)–diopside (Di)–(Mg, Fe, Ca, Na)-carbonates (Carb)–(C-O-H-fluid) system are studied in experiments at 6.0 GPa in the polythermal $Ol_{74}Carb_{18.5}(C-O-H)_{7.5}$-$Omp_{74}Carb_{18.5}(C-O-H)_{7.5}$ section, where $Ol = Fo_{80}Fa_{20}$, Omp (omphacite) = $Jd_{62}Di_{38}$ and Carb = $(MgCO_3)_{25}(FeCO_3)_{25}(CaCO_3)_{25}(Na_2CO_3)_{25}$. The peritectic reaction of olivine and jadeite-bearing melts with formation of garnet has been determined as a physico-chemical mechanism of the ultrabasic–basic evolution of the diamond-forming system. During the process, the $CO_2$ component of the supercritical C-O-H-fluid can react with silicate components to form additional carbonates of Mg, Fe, Ca and Na. The solidus temperature of the diamond-forming system is lowered to 1000–1020 °C by the joint effect of the $H_2O$ fluid and its carbonate constituents. The experimentally recognized peritectic mechanism of the ultrabasic–basic evolution of the diamond-forming system explains the origin of associated paragenetic inclusions of peridotite and eclogite minerals in diamonds, as well as the xenoliths of diamond-bearing peridotites and eclogites of kimberlitic deposits of diamond. Diamond-forming systems have formed with the use of material from upper mantle native peridotite rocks. In this case, the capacity of the rocks to initiate the peritectic reaction of olivine was transmitted with silicate components to diamond-forming systems.

**Keywords:** diamond-forming silicate-carbonate system; C-O-H fluid; peritectic reaction of olivine; ultrabasic–basic evolution; origin of diamond-bearing peridotites and eclogites; high pressure and temperature; experiment

## 1. Introduction

Xenoliths of diamond-bearing peridotites and eclogites as well as inclusions of olivine- and silica-normative minerals in diamonds [1] are indicative of the ultrabasic–basic evolution of diamond-forming silicate-carbonate-(C-O-H-fluid) systems in the depths of the upper mantle. The combined genesis of diamond-bearing rocks and paragenetic inclusions in diamonds occurs in upper mantle diamond-forming chambers [2]. Taken together, these rocks and diamonds were transferred by kimberlitic magma from the mantle chambers through the cumulative centers of the Earth's core to diamond-bearing explosion tubes [3–7]. The upper mantle xenoliths of native peridotites and eclogites, enclosing the diamond-forming chambers, were also captured by kimberlitic magmas [1,8]. It is evident that these rocks were formed as a result of ultrabasic–basic magmatism evolution in a period of crystallization in the global magma ocean with a pyrolite composition [9].

In the absence of experimental evidence, the physico-chemical causes and mechanisms of the ultrabasic–basic evolution of the upper mantle magmatic systems remain unknown [10–13]. H. J. Yoder relates the key problem in the following principle question: how is the crystallization of products of partial melting of garnet peridotite accompanied

by the disappearance of two main phases—olivine and orthopyroxene—while only garnet and clinopyroxene are formed (i.e., eclogite) [14].

The question requires a closer look at the liquidus structure of the multicomponent olivine-clinopyroxene/omphacite-corundum-coesite (Ol-Cpx/Omp-Crn-Coe) system of the upper mantle (Figure 1) [15]. The composition diagram of the multicomponent system (Figure 1a) is a complex mixture of elementary tetrahedrons and simplexes, two of which are ultrabasic—peridotite/pyroxenite $P_1$-peritectic (A) and Ol-Crn-eclogitic $E_1$-eutectic (B)—and three of which are basic—Crn-Ky-eclogitic $E_2$-eutectic (C), Ky-Coe-eclogitic $E_3$-eutectic (D) and Coe-Opx-eclogitic $P_2$-peritectic (E). The complex coordinate framework of the peridotite–eclogite system and a diagram of the liquidus structure are projected onto the divariant section Ol,Cpx-Crn,Cpx/Omp-Coe,Omp, presented in Figure 1b. Each simplex is a bearer of only one invariant eutectic or peritectic point.
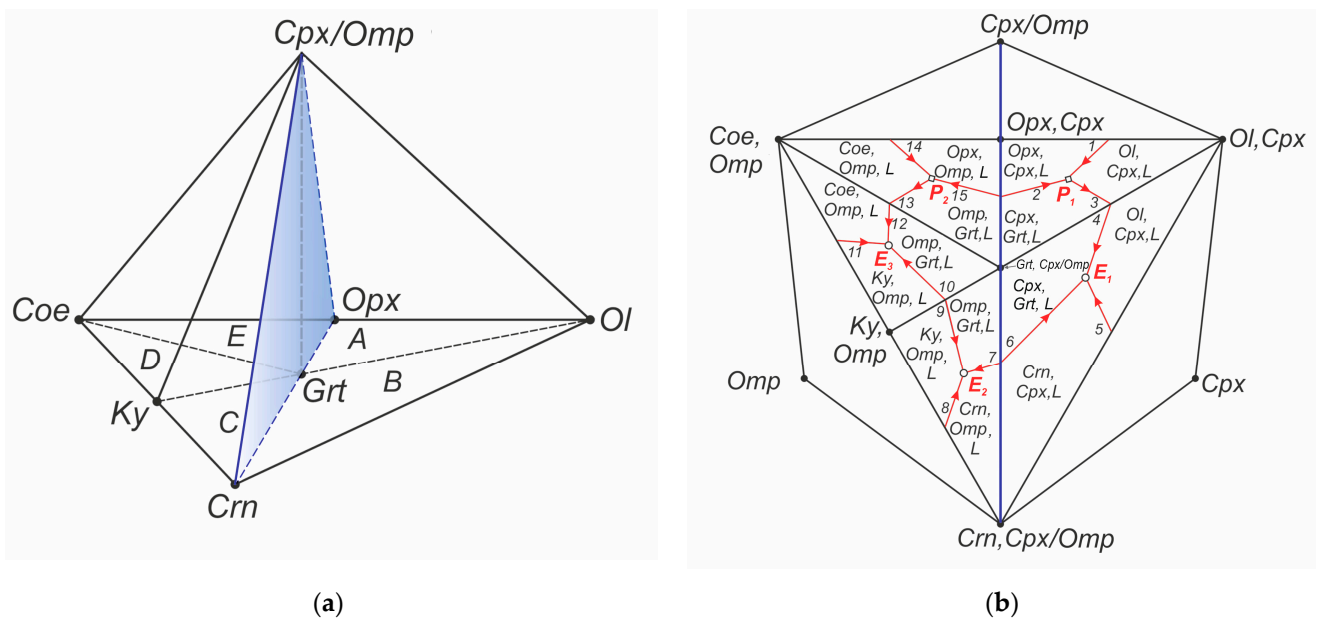


(a)                                        (b)

**Figure 1.** Melting phase relations in a peridotite–eclogite system Ol-Cpx/Omp-Crn-Coe of the upper mantle. (**a**) presents the complex coordinate framework of peridotite–eclogite compositions and its simplexes: (A) peridotite-pyroxenite Ol-Opx-Cpx-Grt, (B) olivine-corrundum eclogite Ol-Crn-Cpx-Grt, (C) corundum-kyanite eclogite Crn-Ky-Omp-Grt, (D) kyanite-coesite eclogite Ky-Coe-Omp-Grt, (E) coesite-orthopyroxene eclogite Coe-Opx-Omp-Grt. The Opx-Cpx/Omp-Crn plane presents the boundary between ultrabasic Ol-Opx-Cpx/Omp-Crn and basic Coe/Omp-Opx-Cpx/Omp-Crn volumes. (**b**) presents the complex liquidus structure of ultrabasic–basic system peridotite-eclogite Ol-Cpx-Crn-Coe, projected from the point Cpx/Omp onto divariant section Ol,Cpx-Crn,Cpx/Omp-Coe,Omp. Peritectic points for Opx are marked as $P_1$ and $P_2$ and eutectic points as $E_1$, $E_2$ and $E_3$. Ultrabasic univariant cotectics: 1—Ol,Cpx,Grt,L; 2—Opx,Cpx,Grt,L; 3—Ol,Cpx,Grt,L; 4—Ol,Cpx,Grt,L; 5—Crn,Cpx,Grt,L; 6—Cpx,Grt,Crn, L. Basic univariant cotectics: 7—Omp,Grt,Crn,L; 8—Crn,Omp,Ky, L; 9—Omp,Ky,Grt,L; 10—Omp,Ky,Grt,L; 11—Ky,Omp,Coe,L; 12—Coe,Omp,Grt,L; 13—Coe,Omp,Grt,L; 14—Coe,Opx,Omp,L; 15—Opx,Omp,Grt,L. Symbols: L, melt; Ol, olivine; Opx, orthopyroxene; Cpx, clinopyroxene; Omp, omphacite; Grt, garnet; Coe, coesite, Crn, corundum, Ky, kyanite.

One distinction between the ultrabasic and basic simplexes of the upper mantle substance is the inner plane Opx-Cpx/Omp-Grt-Crn of the complex diagram. In this case, a univariant cotectic Opx, Cpx, Grt, L of the simplex A (2↔15 with maximum), connecting the ultrabasic $P_1$ and basic $P_2$ peritectics (simplex E), has a temperature maximum (i.e., thermal barrier) at a piercing point in the inner boundary plane. Another thermal barrier exists at a univariant cotectic Cpx/Omp, Grt, Crn, L of simplex B (6↔7) between ultrabasic eutectic $E_1$ and basic eutectic $E_2$ of simplex C.

It should be realized that the boundaries between simplexes represent a peculiar kind of physico-chemical barrier, considering that evolution of the multicomponent system is bounded by its liquidus structure in the volume of separate simplex. Eutectic points with minimal temperatures in the neighboring simplexes as well as temperature maxima in the piercing points also present as thermal barriers in equilibrium under fractional conditions.

Under equilibrium conditions, these thermal barriers eliminate the possibility of the melt evolving from an ultrabasic to a basic composition. In this way, the peritectic point of olivine may not exist, and in consequence, a peritectic disappearance of olivine may not be realized.

Originally, the peritectic reaction of orthopyroxene was affected under conditions of ultrabasic–basic evolution of upper mantle magmatic systems. The reaction has been experimentally studied in the multicomponent olivine-orthopyroxene-clinopyroxene-garnet (Ol-Opx-Cpx-Grt) system in its polythermal $Opx_{51}Ol_{09}Grt_{40}$-$Cpx_{51}Ol_{09}Grt_{40}$ section at 4.0 GPa and 1450 °C [7,16]. As a result, orthopyroxene disappears in the peritectic reaction with the melting and formation of clinopyroxene. A similar simplified reaction of enstatite melting with formation of diopside was studied in experiments at 2.0 GPa and 1650 °C [17] and at 3.0 GPa and 1750 °C [18]. In this case, the peritectic reaction of orthopyroxene is favored over evolution of the upper mantle magmatism only in ultrabasic compositions [15].

As for the olivine problems, a contradiction arises between mineralogical data concerning the probability of its disappearance via the ultrabasic–basic magma evolution on the one hand, and physico-chemical evidence of the impossibility of the olivine peritectic reaction under equilibrium conditions on the other. Nevertheless, an experimental observation of the solid-state reaction of olivine and jadeite with garnet formation [19] allows for the olivine peritectic reaction with jadeite-bearing melt and garnet formation under fractional crystallization conditions.

After the peritectic point $P_1$ Ol, Opx, Cpx, Grt, L (Figure 1b), olivine persists only in compositions of the univariant cotectic Ol, Cpx, Grt, L (3→4 without a maximum) that is directed to the eutectic point $E_1$ of the adjacent ultrabasic simplex. Under conditions of fractional crystallization, the figurative point of the system composition is liable to move within the ultrabasic composition along the univariant cotectic Ol, Cpx, Grt, L to eutectic point $E_1$ if the jadeite component in the system is absent or its concentration is restricted.

Meanwhile, after fractional removal of clinopyroxene, a portion of the jadeite component in the residual melts is first accompanied by the growth in clinopyroxene and then in omphacite components in the general composition of the system. As a result, portion 3 of the univariant cotectic Ol, Cpx, Grt, L is gradually displaced in the direction of the boundary plane Opx-Cpx/Omp-Grt-Crn (Figure 1b). The increase in jadeite concentration also produces the boundary system Jd-Di with completely miscible components. As a result, the new voluminous frontier simplex Ol-Jd-Di-Grt is formed. This simplex forms in the boundary space between the ultrabasic and basic compositions. Thus, the role of the jadeite component in the fractional multicomponent magmatic system changes from an impurity in the ultrabasic peridotites to the system-forming component of basic eclogites.

Thus, under natural conditions, the olivine peritectic reaction represents a key mechanism in the ultrabasic–basic evolution of the upper mantle magmatism. The Earth's gravitational field is favorable to fractional magma evolution and correspondingly to progressive compositional changes in the general system as the residual melts. In these circumstances, the forming minerals break away from the mother melts, whereas low-melting components (including jadeite) accumulate in the melts. Finally, sequential crystallization of clinopyroxene and omphacite results in formation of the continuous jadeite-diopside solid solutions.

Experimental studies of melting phase relations of the upper mantle ultrabasic–basic Ol-Jd-Di system in the Ol-Omp (=$Jd_{62}Di_{38}$) polythermal section (Figures 2 and 3) at 6 GPa reveal a peritectic reaction of olivine and jadeite-bearing melt with formation of garnet [20]. As a result, a transition to the basic univariant cotectic Omp, Grt, L is observed with

formation of bimineral eclogites. It can be seen that the liquidus structure of the Ol–Di–Jd–(reactionary Grt) system (Figure 3) is of special interest as a peculiar "physico-chemical bridge" between the ultrabasic peridotite-pyroxenite and basic eclogite rocks of the upper mantle garnet-peridotite facies. These results reveal not only genetic relations between ultrabasic and basic rocks but also physico-chemical mechanisms of continuous fractional magmatic evolution and petrogenesis from olivine-bearing peridotites to silica-saturated eclogites. These data provide an explanation for the continual petrochemical trends of rock-forming components in clinopyroxenes/omphacites and garnets of differentiated rocks of garnet-peridotite facies [21].
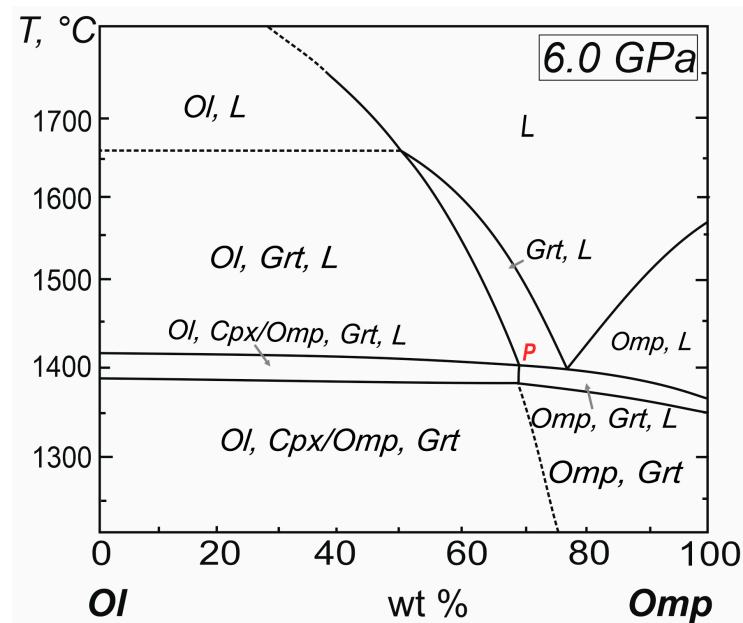


**Figure 2.** Melting phase relations in ultrabasic–basic Ol-Jd-Di system for its Ol (=$Fo_{80}Fa_{20}$)–Omp (=$Di_{38}Jd_{62}$) polythermal section at 6.0 GPa [20]. Symbols: P, peritectic point; L, melt; Ol, olivine; Fo, forsterite; Fa, fayalite; Omp, omphacite; Jd, jadeite; Di, diopside; Grt, garnet.
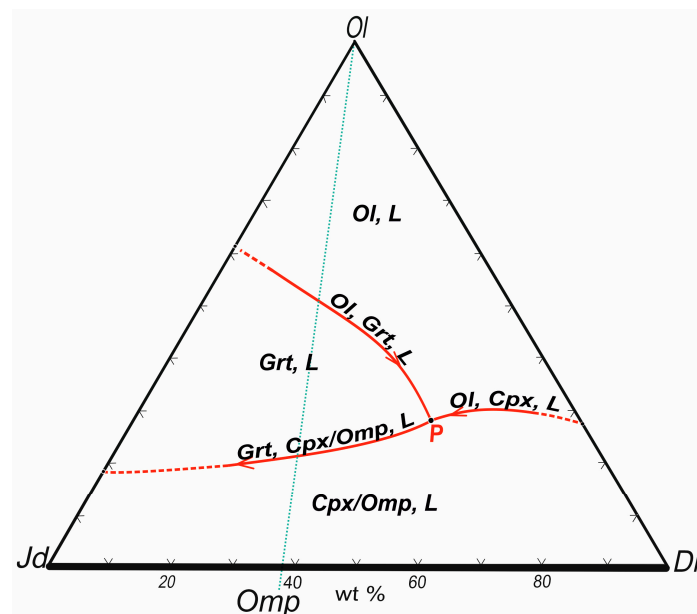


**Figure 3.** Peritectic liquidus in the ultrabasic–basic Ol–Jd–Di system [20]. The location of the Ol-Omp polythermal section is shown by a dotted line. Symbols: P, peritectic point; L, melt; Ol, olivine; Cpx, clinopyroxene; Omp, omphacite; Jd, jadeite; Di, diopside; Grt, garnet.

The fluid-bearing system Ol-Di-Jd-(C-O-H) in the $Ol_{95}(C-O-H)_{05}$–$Omp_{95}(C-O-H)_{05}$ polythermal section [22] (Figures 4 and 5) was also investigated experimentally at 6 GPa. It was found that a super-critical C-O-H fluid (with content of 5.0 wt.%) influences the composition and temperature of the peritectic reaction of olivine and jadeite-bearing melt with formation of garnet. This reaction controls the closing stage of the fractional ultrabasic–basic evolution of upper mantle magmatic melts. According to experimental evidence, the reaction retains its significance, since the C-O-H fluid components do not induce changes in melting phase relations of the ultrabasic–basic olivine-jadeite-diopside-(reactionary Grt)-(C-O-H-fluid) system at 6 GPa. Along with this, metasomatic $CO_2$ carbonization of silicates and solvation of $H_2O$ fluid in completely mixed silicate–carbonate melts were found. It also was found that C-O-H fluid favorably influences the temperature decreases of liquidus and solidus boundaries, respectively, from 1660 to 1580 °C and from 1420 to 1290 °C, as well as increases the olivine component in the olivine peritectic reaction by 10 wt.%.
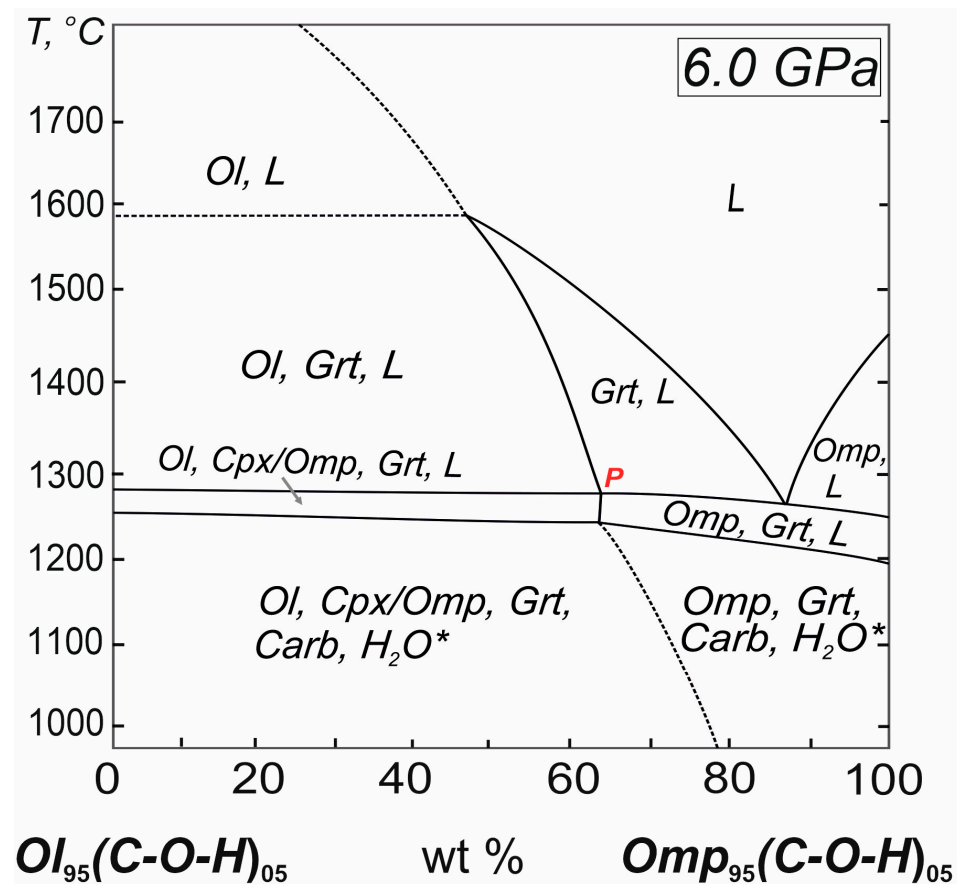


**Figure 4.** Melting relations of the $Ol_{95}(C-O-H)_{05}$–$Omp_{95}(C-O-H)_{05}$ polythermal section in the ultrabasic–basic Ol-Jd–Di–(C-O-H-fluid) system at 6.0 GPa [22]. Symbols: P, peritectic point; L, melt; Ol, olivine (=$Fo_{80}Fa_{20}$); Omp, omphacite (=$Di_{38}Jd_{62}$); Cpx, clinopyroxene; Grt, garnet; Carb, carbonate mix $(MgCO_3)_{25}(FeCO_3)_{25}(CaCO_3)_{25}(Na_2CO_3)_{25}$; $H_2O^*$, supercritical water.
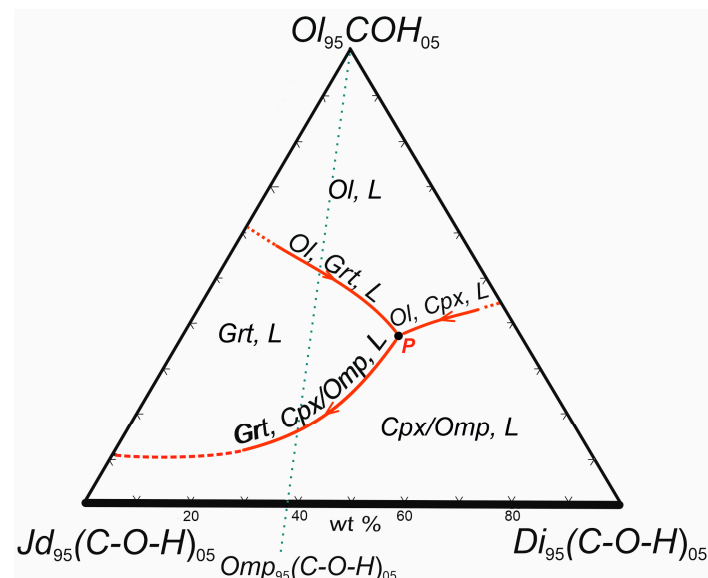
**Figure 5.** Structure of equilibrium peritectic liquidus of the ultrabasic–basic Ol–Jd–Di–(C-O-H-fluid) system [22]. The location of the $Ol_{95}(C-O-H)_{05}$–$Omp_{95}(C-O-H)_{05}$ polythermal section is shown by a dotted line. Symbols: P, peritectic point; L, melt; Ol, olivine; Omp, omphacite; Cpx, clinopyroxene; Grt, garnet.

Thus, peritectic reactions of orthopyroxene and olivine with melts lead to conversion of the ultrabasic peridotite mineral system into the basic eclogitic one under conditions of the upper mantle fractional magmatic evolution. It is essential that xenoliths of diamond-bearing peridotites and eclogites in kimberlitic explosion tubes as well as inclusions of the olivine- and silica-normative minerals in diamonds are able to influence the possibility of an ultrabasic–basic evolution of the upper mantle diamond-forming multicomponent silicate-carbonate-(C-O-H-fluid) system. However, the problem has still not been studied with physico-chemical experiments.

Meanwhile, the genesis of diamond and associated mineral phases is realized in the upper mantle diamond-forming chambers according to the mantle-carbonatite theory [7]. Under these conditions, the parental silicate-carbonate media of diamonds and genetically associated phases are formed by streams of C-O-H-fluids reacting with native silicate rocks of the upper mantle. The C-O-H fluid inclusions in diamonds and xenolithic minerals testify to its presence in the mantle at pressures up to 10 GPa [23]. In this case, the fluid compositions are variable, from $CO_2$ enriched with $H_2O$ to $H_2O$ enriched with $CO_2$ [24]. Genetic links between the mantle silicate and diamond-forming silicate-carbonate systems originate in metasomatic reactions of $CO_2$ with upper mantle silicate minerals, resulting in formation of carbonate minerals and melts. Then, the same mantle minerals and graphite were dissolved in carbonate and completely miscible silicate-carbonate melts containing C-O-H fluid. As a result, chambers of diamond-forming silicate-carbonate-(C-O-H-fluid)-carbon melts were formed. In these processes, the peritectic reaction of olivine and jadeite-bearing melt with formation of garnet moved to take place in the silicate components of the diamond-forming system. Carbonate-bearing diamond-forming melts are effective solvents of solid carbon phases, producing carbon-saturated diamond solutions. Oversaturated diamond silicate-carbonate melt solutions of carbon are generated at lower temperatures in the diamond-forming chamber. This leads to the spontaneous crystallization of diamond. As a result, diamonds with paragenetic mineral inclusions as well as diamond-bearing peridotites and eclogites are formed [2]. Consolidated diamond-bearing upper mantle chambers come into existence over extended geological periods.

The ultrabasic–basic melt conversion of multicomponent diamond-forming melts of the olivine-orthopyroxene-clinopyroxene-garnet-(Mg-Fe-Ca-Na-carbonates)-(C-O-H-fluid) system under upper-mantle *PT* conditions has not been experimentally investigated.

The main objectives of this work are the following:

(1)　Experimental studies at 6.0 GPa of liquidus phase relations in the diamond-forming olivine-jadeite-diopside-(Mg-Fe-Ca-Na-carbonates)-(C-O-H-fluid) system with 7.5 wt.% of fluid. Therewith, the possibility of the peritectic reaction of olivine and jadeite-bearing melt with formation of garnet will be established.

(2)　Evaluation of the influence of carbonate components and increased content of the super-critical (C-O-H) fluid on phase relations and *PT* conditions of the diamond-forming system.

(3)　Substantiation of a physico-chemical scenario for fractional ultrabasic–basic evolution of the diamond-forming silicate-carbonate-(C-O-H-fluid) melts and formation of diamond-bearing rocks and diamonds with paragenetic inclusions of ultrabasic and basic minerals.

## 2. Experimental, Analytical and Physico-Chemical Procedures

A complex approach to the solution of the genetic problems of geochemistry, mineralogy and petrology of the Earth's mantle is used in physico-chemical experiments. This may be realized with a combination of experimental methods at high pressure and temperature, micro-analytical diagnosis of experimental phases and knowledge of the physical chemistry of multicomponent multiphase systems.

### 2.1. Experimental Equipment and Methods

Experimental studies were performed in an anvil-with-hole toroidal high pressure high-temperature apparatus with a cell made of lithographic limestone and an isothermal tubular heater of 7.2 mm in height and 7.0 mm in diameter (Figure 6) [16]. Experimental samples were placed in hermetically sealed Pt ampules of 4.0 mm in height and 5.0 mm in diameter. The Pt ampules were placed into the heater with mixed MgO and BN isolation. The pressure was determined using standard polymorphism of Bi (at 2.55 GPa) and Tl (at 3.67 GPa) with an accuracy $\pm 0.25$ GPa. The temperature was regulated in the limits of $\pm 2\,^{\circ}$C and measured by a $Pt_{30}Rh_6$ thermocouple with an accuracy $\pm 10\,^{\circ}$C. All runs were completed by a quenching procedure with a rate of ~300 °C/s.
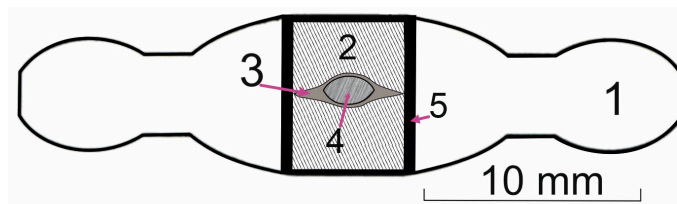


**Figure 6.** A schematic drawing of the assembly design for experiments of the anvil-with-hall (toroidal) apparatus: (1) container (lithographic limestone); (2) capsule insulation (a mixture of MgO and hexagonal BN); (3, 4) starting sample in the Pt capsule; (5); tubular heater (graphite).

### 2.2. Starting Materials

A gel mixture of olivine (Ol = $(Fo_{80}Fa_{20})$ = $(Mg_2SiO_4)_{80}(Fe_2SiO_4)_{20}$) and omphacite (Omp = $(Jd_{62}Di_{38})$ = $(NaAlSi_2O_6)_{62}(CaMgSi_2O_6)_{38}$) and the chemical reagent of carbonates (Carb = $(MgCO_3)_{25}(FeCO_3)_{25}(CaCO_3)_{25}(Na_2CO_3)_{25}$) were used in the experimental study of the liquidus structure of the Ol–Jd–Di–(Mg-Fe-Ca-Na-carbonates)–(C-O-H-fluid) system at 6 GPa. A supercritical (C-O-H) fluid was generated in situ by breaking down dihydrate oxalic acid in the following reaction: $H_2C_2O_4 \cdot 2H_2O \rightarrow 2CO_2 + 2H_2O + H_2$. In this case, the hot walls of the hermetic Pt ampules are permeable for hydrogen diffusion. A mix of supercritical $CO_2$ and $H_2O$ fluids is left in place.

### 2.3. Critical PTN-Surface of the $H_2O$-$CO_2$ System

A phase diagram of the $H_2O$-$CO_2$ system at 6 GPa is presented in Figure 7 [25] together with the subsolidus $\beta$-$H_2CO_3$ phase from the data in [26]. A subsolidus assembly of $H_2O$

(ice VII) + $\beta$-$H_2CO_3$ melts at the eutectic point at 220 °C with formation of a completely mixed liquid phase $L_{H_2O>CO_2}$ and two $L_{H_2O>CO_2}$ + $H_2O$ (ice VII) and $L_{H_2O>CO_2}$ + $\beta$-$H_2CO_3$ phase fields. At a temperature of ~250 °C, the peritectic reaction of $\beta$-$H_2CO_3$ takes place with formation of $L_{H_2O>CO_2}$ + $CO_2$ (ice) which is stable up to 360 °C. At higher temperatures, the phase field $L_{CO_2>H_2O}$ + $CO_2$ (ice) is formed, together with the dome-shaped field of the unmixing liquids $L_{H_2O>CO_2}$ + $L_{CO_2>H_2O}$ with the temperature maximum of ~440 °C at 65 wt.% of $CO_2$. Consequently, the critical *PTN*-surface of the $H_2O$-$CO_2$ system is formed (where N is the composition). At higher temperatures, supercritical $H_2O$ and $CO_2$ fluids are completely miscible.
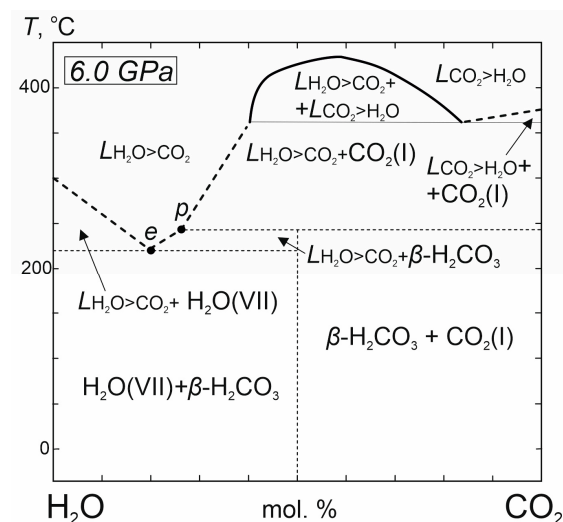


**Figure 7.** Temperature–composition phase relations of the $H_2O$-$CO_2$ system at a pressure of 6 GPa [25] with solid phase $\beta$-$H_2CO_3$ [26].

### 2.4. Analytical Methods

The experimental samples were studied over both polished and unpolished surfaces with the methods of scanning electron microscopy and electron microanalysis using a CamScanMV230 electron microscope (VEGA TS 5130MM) with an energy-dispersive Link INA Energy-350 analyzer (with an accelerating voltage of 20 kV). The size of the electron probe was 115–140 nm and up to 60 nm in a scanning mode; the excitation region is up to 5 μm in diameter. Quartz, albite, MgO, $Al_2O_3$, wollastonite and Mn, Cr, Ti and Fe metals were used as standards.

The method of Raman spectroscopy was also used. The KR spectra of experimental samples were taken using an Acton SpectraPro-2500i spectrometer with a CCD Pixis2K detector and an Olympus microscope with a solid-phase laser (wavelength of 532 nm, spot ~5 μm in diameter, excitation intensity of ~0.7 мВт).

Analyses were performed at the D.S. Korzhinskii Institute of Experimental Mineralogy of the Russian Academy of Sciences.

### 2.5. Methods of Physical Chemistry of Multicomponent Systems

The physical and chemical mechanisms of the origin and evolution of magmatic minerals and rocks of the Earth's mantle can be revealed by experimental studies of melting phase relations of multicomponent multiphase systems. Their compositions reflect the major components of the deep-seated substances. Physical chemistry methods of multicomponent systems [27,28] may be applied to solve experimental problems and used in investigation and analysis of scientific results. These lines of attack are effective in studies of physico-chemical mechanisms of ultrabasic–basic evolution of upper-mantle magmatic and diamond-forming systems. In this case, the peritectic reactions of orthopyroxene and melt with formation of clinopyroxene as well as olivine and jadeite-bearing melt with formation of garnet have a dominant role [2,15,16,19,21].

Diagrams of the multicomponent multiphase system are composed of the simplest diagrams and simplexes with only one invariant eutectic or peritectic point. Under equilibrium conditions, their inter-simplex boundaries present physico-chemical barriers. A fractional removal of the forming solid phases changes the general system composition which becomes equal to the remaining melts. Therewith, the transfer of the figurative points of the system composition to neighboring simplexes is possible because their peritectic points are combined with the temperature-reduced univariant eutectics. The method of measuring two polythermic sections makes it possible to experimentally research the inter-simplex fractional ultrabasic–basic crystallization. The Rhines phase rule [27] controls the topological correctness of the multicomponent melt diagrams. The diagrams reveal the evolution mechanisms of the upper mantle magmatic and diamond-forming systems.

## 3. Experimental Studies

The melting phase relations of the diamond-forming olivine (Ol)–jadeite (Jd)–diopsite (Di)-$MgCO_3$-$FeCO_3$-$CaCO_3$-$Na_2CO_3$-(C-O-H-fluid) system were experimentally studied at 6.0 GPa in the $Ol_{74}Carb_{18.5}(C-O-H)_{7.5}$-$Omp_{74}Carb_{18.5}(C-O-H)_{7.5}$ polythermal section, where $Ol = Fo_{80}Fa_{20}$, $Omp = Jd_{62}Di_{38}$ and $Carb = (MgCO_3)_{25}(FeCO_3)_{25}(CaCO_3)_{25}(Na_2CO_3)_{25}$. The content of the starting (C-O-H) fluid was 7.5 wt.%. Choosing this section permits to trace the change in system composition from an ultrabasic olivine-bearing to a basic silica-saturated system. Moreover, estimation of the transfer from clinopyroxenes, enriched with the diopside component, to omphacites, enriched with the jadeite component, is made possible.

The diagram of the melting phase relations for the system under experimental study was constructed (Figure 8) using the electron microscopic (Figure 9) and analytical (Table 1) data. This permits to determine the liquidus structure of the diamond-forming system and the composition of the invariant point for the olivine peritectic reaction, which is a key physico-chemical mechanism of the fractional ultrabasic–basic evolution of diamond-forming silicate-carbonate melts.
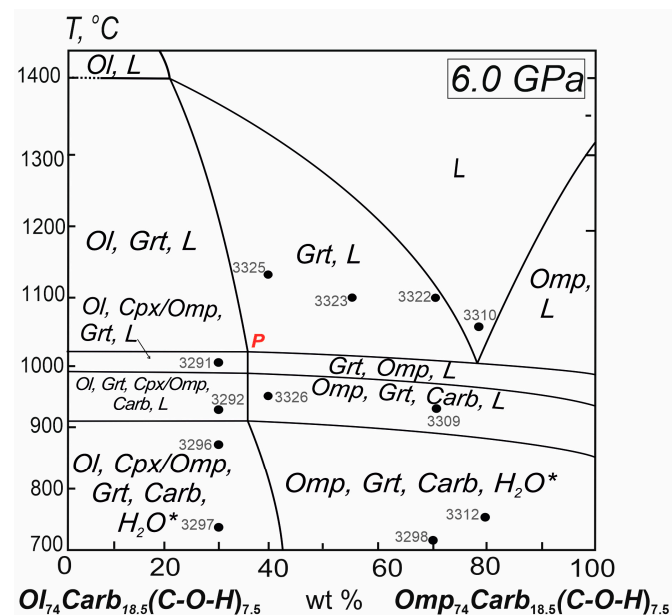


**Figure 8.** Melting relations of the ultrabasic–basic diamond-forming Ol-Jd–Di–Carb–(C-O-H-fluid) system in its $Ol_{74}Carb_{18.5}(C-O-H)_{7.5}$–$Omp_{74}Carb_{18.5}(C-O-H)_{7.5}$ polythermal section at 6.0 GPa. Symbols: P, peritectic point, L, melt; Ol, olivine; Fo, forsterite; Fa, fayalite; Omp, omphacite; Grt, garnet; Carb, carbonates; $H_2O^*$, supercritical water. Numbered points correspond to experimental compositions (in the table).
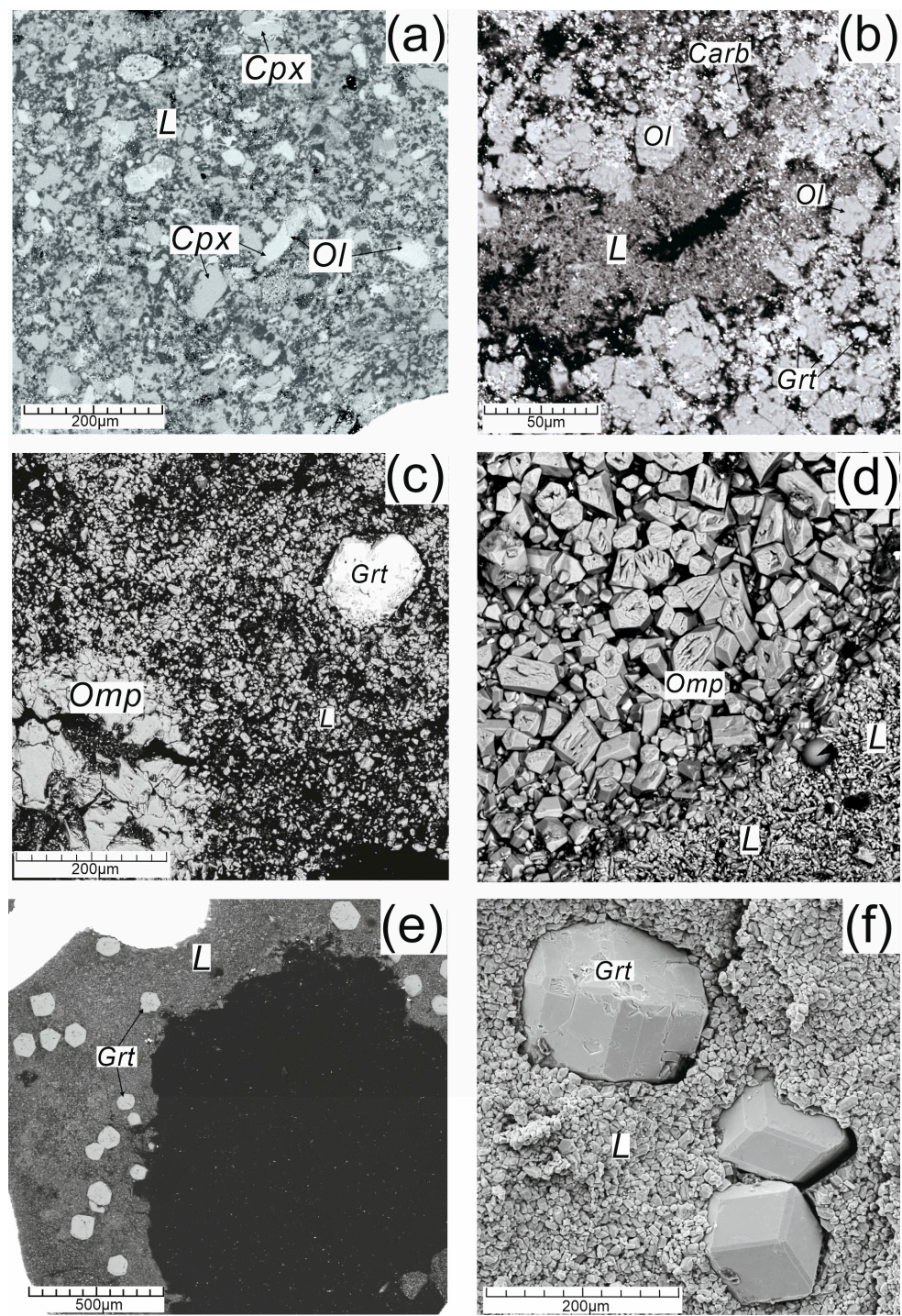
**Figure 9.** SEM images of the sample of the ultrabasic (**a**,**b**) and basic (**c**–**f**) compositions. Symbols: L, melt; Ol, olivine; Omp, omphacite; Cpx, clinopyroxene; Grt, garnet; Carb, carbonates.

**Table 1.** Table of experimental conditions and compositions of experimental phases.

| N° Sample | Starting Composition | T, °C | Duration, min | Phase | Chemical Analyses of Experimental Phases, wt.% of Elements Oxides | | | | | | | |
|---|---|---|---|---|---|---|---|---|---|---|---|---|
| | | | | | $SiO_2$ | $Al_2O_3$ | MgO | FeO | CaO | $Na_2O$ | $CO_2$ * | Total |
| 3291 | $[(Ol_{80}Omp_{20})_{80}$ $Carb_{20}]_{92.5}COH_{7.5}$ | 1020 | 95 | Ol | 38.75 | 0.30 | 41.71 | 16.68 | 0.09 | 0.03 | - | 96.80 |
| | | | | Grt | 38.93 | 20.85 | 11.96 | 20.67 | 6.04 | 0.18 | - | 98.65 |
| | | | | Omp | 53.90 | 2.79 | 12.38 | 8.13 | 17.54 | 3.74 | - | 98.47 |
| | | | | L | 13.72 | 0.43 | 2.77 | 19.99 | 17.39 | 14.34 | 31.36 | 100.00 |
| 3292 | $[(Ol_{80}Omp_{20})_{80}$ $Carb_{20}]_{92.5}COH_{7.5}$ | 930 | 120 | Cpx | 57.36 | 6.63 | 12.44 | 8.26 | 13.38 | 6.60 | - | 104.67 |
| | | | | Ol | 28.02 | 0.24 | 33.69 | 27.73 | 0.04 | 0.47 | - | 90.19 |
| | | | | L | 14.34 | 2.77 | 13.72 | 0.55 | 17.36 | 19.75 | 31.51 | 100.00 |
| | | | | L | 10.90 | 1.19 | 31.32 | 8.27 | 3.38 | 0.84 | 44.10 | 100.00 |
| 3296 | $[(Ol_{80}Omp_{20})_{80}$ $Carb_{20}]_{92.5}COH_{7.5}$ | 875 | 60 | Ol | 30.71 | 0.37 | 28.38 | 38.61 | 0.14 | 0.75 | - | 99.28 |
| | | | | Omp | 55.19 | 11.26 | 7.73 | 5.07 | 8.97 | 9.68 | - | 97.90 |
| | | | | Mg,Fe-carb | - | - | 41.12 | 13.66 | 6.37 | - | 38.85 | 100.00 |
| 3297 | $[(Ol_{80}Omp_{20})_{80}$ $Carb_{20}]_{92.5}COH_{7.5}$ | 740 | 90 | Ol | 30.28 | - | 41.08 | 21.13 | - | 0.75 | - | 93.24 |
| | | | | Omp | 55.43 | 13.90 | 7.17 | 4.69 | 7.29 | 11.26 | - | 99.74 |
| | | | | Carb | 1.72 | - | 38.65 | 7.30 | 0.30 | 2.11 | 49.92 | 100.00 |
| 3323 | $[(Ol_{45}Omp_{55})_{80}$ $Carb_{20}]_{92.5}COH_{7.5}$ | 1100 | 90 | Grt | 40.51 | 22.08 | 12.16 | 11.05 | 11.28 | 3.03 | - | 100.11 |
| | | | | L | 3.61 | 0.14 | 1.63 | 0.66 | 1.02 | 22.98 | 69.96 | 100.00 |
| 3325 | $[(Ol_{40}Omph_{60})_{80}Carb_{20}]_{92.5}COH_{7.5}$ | 1130 | 90 | Grt | 40.25 | 21.02 | 9.18 | 12.28 | 17.14 | 0.2 | - | 100.07 |
| | | | | L | 42.64 | 9.21 | 8.86 | 5.47 | 13.31 | 3.47 | 17.04 | 100.00 |
| 3326 | $[(Ol_{40}Omph_{60})_{80}Carb_{20}]_{92.5}COH_{7.5}$ | 950 | 90 | Grt | 40.44 | 21.21 | 9.74 | 12.24 | 15.91 | 0.11 | - | 99.65 |
| | | | | L | 23.38 | 0.04 | 0.04 | 0.11 | 3.63 | 34.89 | 37.91 | 100.00 |
| | | | | Omp | 56.22 | 9.22 | 11.48 | 0.79 | 16.21 | 5.04 | - | 98.96 |
| | | | | Carb | 9.13 | 0.71 | 1.14 | 0.53 | 2.40 | 38.36 | 47.73 | 100.00 |
| 3322 | $[(Ol_{30}Omp_{70})_{80}$ $Carb_{20}]_{92.5}COH_{7.5}$ | 1100 | 90 | Grt | 40.83 | 21.24 | 6.02 | 13.6 | 17.71 | 0.14 | - | 99.54 |
| | | | | L | 44.28 | 6.81 | 7.77 | 3.08 | 10.71 | 5.49 | 21.86 | 100.00 |
| 3309 | $[(Ol_{30}Omp_{70})_{80}$ $Carb_{20}]_{92.5}COH_{7.5}$ | 950 | 90 | Grt | 37.11 | 16.50 | 19.11 | 3.83 | 21.39 | 0.43 | - | 98.37 |
| | | | | Omp | 51.14 | 1.97 | 14.41 | 6.30 | 20.38 | 4.91 | - | 99.11 |
| | | | | Ca,Na-carb | 0.03 | 0.11 | 0.77 | 1.53 | 15.88 | 21.13 | 60.55 | 100.00 |
| | | | | Na-carb | 2.93 | 0.36 | 6.85 | 5.90 | 2.40 | 24.60 | 56.96 | 100.00 |
| | | | | Carb | 4.50 | 0.79 | 14.78 | 14.99 | 10.76 | 12.58 | 41.60 | 100.00 |
| | | | | Carb | 1.28 | 1.13 | 28.04 | 22.22 | 2.35 | 0.64 | 44.34 | 100.00 |
| | | | | L | 28.63 | 0.85 | 11.11 | 6.59 | 12.62 | 7.10 | 33.10 | 100.00 |
| 3298 | $[(Ol_{30}Omp_{70})_{80}$ $Carb_{20}]_{92.5}COH_{7.5}$ | 710 | 90 | Omp | 57.89 | 17.44 | 3.65 | 2.84 | 4.16 | 13.08 | - | 99.06 |
| | | | | Arg | 0.18 | 0.08 | 0.22 | 0.00 | 55.08 | 0.37 | 44.07 | 100.00 |
| | | | | Mgs | 2.10 | 0.69 | 38.44 | 5.80 | 1.64 | 0.96 | 50.37 | 100.00 |
| 3310 | $[(Ol_{20}Omp_{80})_{80}$ $Carb_{20}]_{92.5}COH_{7.5}$ | 1060 | 60 | L | 25.06 | 6.18 | 17.26 | 2.42 | 6.63 | 17.94 | 24.51 | 100.00 |
| 3312 | $[(Ol_{20}Omp_{80})_{80}$ $Carb_{20}]_{92.5}COH_{7.5}$ | 790 | 90 | Omp | 48.85 | 1.55 | 12.35 | 6.18 | 19.70 | 7.87 | - | 96.50 |
| | | | | Carb | - | - | 0.66 | 0.89 | 49.91 | 4.87 | 43.67 | 100.00 |

* $CO_2$-counted.

Intense processes of carbonatization of the silicate components of minerals and melts of the diamond-forming system proceed under the action of the $CO_2$ components from the supercritical C-O-H fluid. This is evidenced by numerous small-sized quenched grains of Na, Mg, Fe and Ca carbonates amongst clinopyroxenes and omphacites as well as inclusions in garnets. The newly formed carbonates add themselves to the carbonate constituent of the diamond-forming system. The reactions of $CO_2$ fluid with olivine and other rock-forming minerals of the upper mantle with formation of Mg-carbonate are known [29,30]. The supercritical C-O-H-fluid becomes enriched with the $H_2O$ component after binding of $CO_2$ in the formed carbonates.

The compositions of the experimental phases of olivine are variable, with an average value of $(Mg_2SiO_4)_{58}(Fe_2SiO_4)_{42}$. The content of the jadeite component $NaAlSi_2O_6$ in the clinopyroxene-omphacite solid solutions is changeable within 10–67 wt.%, and the

concentration of the pyrope component in the grossular-pyrope garnets corresponds to 9.7–46.0 wt.%. Garnets are the product of the peritectic reaction of olivine and jadeite-bearing silicate-carbonate melts with dissolved $H_2O$ fluid. Single garnet crystals may be as large as 200 µm after spontaneous crystallization (Figure 9c,e,f).

The peritectic reaction of olivine (P) at 6.0 GPa and 1020 °C after study the $Ol_{74}Carb_{18.5}$ $(C-O-H)_{7.5}$-$Omp_{74}Carb_{18.5}(C-O-H)_{7.5}$ polythermal section of the Ol-Jd–Di–Carb–(C-O-H-fluid) system was revealed (Figure 8). It is necessary to turn our attention to the peritectic reaction in the phase diagram of the multicomponent system being represented as a quasi-invariant "point". Actually, it is a short univariant line parallel to the temperature coordinate. Respectively, the combined univariant ultrabasic Ol,Grt,Cpx/Omp,L and basic Grt,Omp,L cotectics appear as narrow divariant fields. The topological peculiarities are in agreement with Rhines' phase rule for multicomponent systems [27].

On the basis of the experimental data, a diagram of the liquidus structure of the diamond-forming $Ol_{74}Carb_{18.5}(C-O-H)_{7.5}$-$Jd_{74}Carb_{18.5}(C-O-H)_{7.5}$-$Di_{74}Carb_{18.5}(C-O-H)_{7.5}$ system was constructed (Figure 10). The auxiliary dotted thin line over the diagram demonstrates the relative position of the polythermal section (see Table 1).
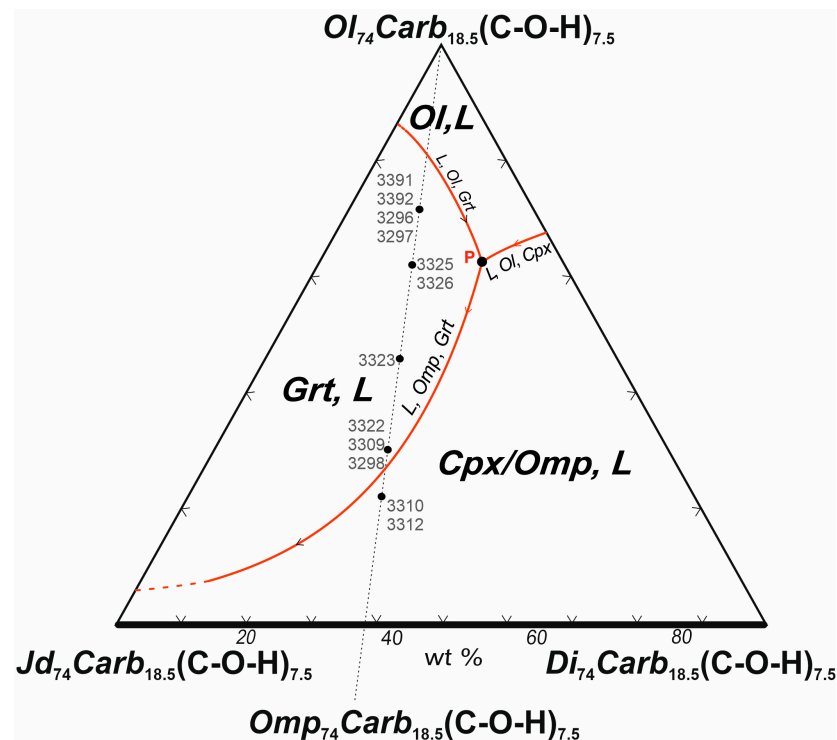


**Figure 10.** The peritectic point of the ultrabasic–basic diamond-forming Ol–Jd–Di–Carb-(C-O-H-fluid) system. The position of the polythermal section $Ol_{74}Carb_{18.5}(C-O-H)_{7.5}$–$Omp_{74}Carb_{18.5}(C-O-H)_{7.5}$ is shown by the dotted line. Numbered black points are experimental compositions (see the table). Symbols: P, peritectic point; L, melt; Ol, olivine; Omp, omphacite; Cpx, clinopyroxene; Grt, garnet; Carb, carbonate mix.

The peritectic point P of the diamond-forming system is shifted to the boundary of the olivine-bearing composition when compared to the similar upper mantle olivine-jadeite-diopside-(C-O-H-fluid) system with a 5.0 wt.% content of C-O-H fluid (Figure 6) [22]. Therewith, the solidus temperature of the diamond-forming system decreased by 270 °C down to 1000–1020 °C relative to the upper mantle silicate system $Ol_{95}(C-O-H)_{05}$–$Omp_{95}(C-O-H)_{05}$.

According to experimental data, supercritical $H_2O$ fluid is liberated upon crystallization of the diamond-forming silicate-carbonate fluid Ol–Jd–Di–Carb-(C-O-H-fluid) and the upper mantle Ol–Jd–Di-(C-O-H-fluid) native systems [22]. In these cases, $H_2O$ fluid can form self-dependent subsolidus phases.

From a geochemical point of view, merging of both the diamond-forming silicate-carbonate and the upper mantle silicate systems is accompanied by them splitting into magmatic and hydrothermal systems coexisting in the open state.

According to preliminary data, evidence of hydrothermal activity is observed in the subsolidus phase assembly of the diamond-forming system in the form of embryonic geode-like structures filled with silicate and carbonate phases (Figure 11a). The reaction of the $H_2O$ fluid and carbonates with formation of water-bearing carbonate mineral nesquehonite ($MgCO_3 \cdot 3H_2O$) was also established by self-dependent minerals and paragenetic inclusions in diamond (Figure 11b).



(**a**)



(**b**)

**Figure 11.** SEM images of the results of hydrothermal activity under subsolidus conditions of the diamond-forming Ol–Jd–Di–Carb-(C-O-H-fluid) system at 6.0 GPa: (**a**) geode-like structures; (**b**) inclusion of nesquehonite $CaCO_3 \cdot 3H_2O$ in garnet. Symbols: Omp, omphacite; Grt, garnet; Carb, carbonates; Mgs, magnesite; Arg, aragonite; Nes, nesquehonite.

## 4. Discussion

An investigation into the liquidus structure of the multicomponent diamond-forming silicate-carbonate-(C-O-H-fluid) system via physico-chemical experiments at 6.0 GPa revealed a peritectic reaction of olivine and jadeite-bearing melt with formation of garnet. Therewith, the key role of this reaction in the fractional ultrabasic–basic evolution of the parental melts for diamond and genetically associated minerals was demonstrated. As a result, a rational physico-chemical explanation has been given for the genesis of diamond-bearing peridotites and eclogites, as well as the paragenesis of diamonds with of ultrabasic and basic mineral inclusions.

The importance of the peritectic reaction of olivine and jadeite-bearing melt with formation of garnet in the fractional ultrabasic–basic evolution of the upper mantle magmatic systems and the genesis of native peridotite and eclogite rocks has been demonstrated in previous experimental studies [20,22]. It is probable that the physico-chemical mechanisms and processes took place at the time of the crystallization of the global magmatic ocean at upper mantle depths.

An analysis of mineralogical and experimental information, related to the upper mantle silicate rocks and diamond-forming silicate-carbonate materials, has revealed the physico-chemical mechanisms of the ultrabasic–basic evolution. A clearer view of the genetic links between diamond-forming systems and upper mantle native rocks has been obtained. The principal conclusion lies in the fact that after formation of the diamond-forming systems with the use of upper mantle native peridotite rocks, the capability of the native peridotites for the peritectic reaction of olivine was passed on to the silicate components of the diamond parental medium.

Hence, the diamond-forming processes represent the combined crystallization of diamonds and associated phases with the formation of paragenetic mineral inclusions in diamonds. The inclusions are analogous to the upper mantle minerals that were recrystallized in the completely mixed silicate-carbonate diamond-forming melts. Rock-forming minerals of the diamond-bearing rocks originated similarly and are estimated to be recrystallized analogues of the mantle minerals.

The origin of diamond-forming systems in the Earth's mantle is among the principal questions for the mantle-carbonatite theory of diamond genesis [7]. Under these conditions, the systems' compositions must be suited the creation criteria for diamonds and their paragenetic and xenogenetic mineral phases [30]. These requirements relate to diamond-bearing peridotites and eclogites as well as syngeneic mineral inclusions in diamonds.

The $CO_2$ component of ascending supercritical C-O-H fluid provides the metasomatic carbonation reactions of the rock-forming mantle minerals of peridotites (olivine, orthopyroxene, clinopyroxene and garnet) and/or eclogites (omphacite and garnet). As a result, diamond parental silicate-carbonate (Mg, Fe, Ca and Na) melts with dissolved elemental carbon are formed. The components of the mantle minerals are dissolved in the carbonate melts, forming the silicate constituent of the diamond-forming medium. The origin of the carbon source has been retraced by isotopic data from the accretion of the carbonaceous chondrites in mantle-native carbon-bearing rocks [31–33]. As a result of these reactions, completely miscible silicate-carbonate melts formed. The silicate-carbonate melts, just like the carbonate ones, are the effective solvents of carbon that result in diamond-forming silicate-carbonate-carbon melt solutions. As this takes place, the silicate constituent of the melt solutions retains the ability to induce peritectic reactions of orthopyroxene and olivine. These reactions make the ultrabasic–basic transfer of the diamond-forming melts under conditions of fractional crystallization possible.

The content of the supercritical $H_2O$ fluid dissolved in silicate-carbonate melts becomes dominant in relation to the remaining $CO_2$ fluid. Under solidus *PT* conditions, the completely mixed silicate-carbonate melts with dissolved $H_2O$ fluid crystallize, forming subsolidus silicate and carbonate minerals. At the same time, the components of the $H_2O$ fluid are separated, with formation of their own supercritical phase. This phase becomes the chemically active agent of hydrothermal processes. In this way, a supercritical hydrothermal system has formed that is open with respect to the enclosing silicate-carbonate subsolidus association of the diamond-forming system and is capable of physico-chemical reactions with the system.

It is probable that supercritical $H_2O$ fluid and the carbonate components are responsible for a decrease in the solidus temperature to 1000–1020 °C compared to the diamond-forming system.

## 5. Conclusions

Experimental studies at 6.0 GPa of the multicomponent diamond-forming olivine-jadeite-diopside-(Mg, Fe, Ca and Na carbonate)-(C-O-H-fluid) system were carried out under *PT* conditions where diamond is stable and with a content of the C-O-H-fluid of 7.5 wt.%. The peritectic reaction of olivine and jadeite-bearing silicate-carbonate melt with formation of garnet was established. As the key physico-chemical mechanism, the "garnetization of olivine" reaction causes the ultrabasic–basic evolution of the completely miscible silicate-carbonate melts. These results provide an explanation for the genesis of the ultrabasic and basic mineral associations that are characteristic of the paragenetic inclusions in diamond and diamond-bearing peridotites and eclogites.

The influence of the C-O-H-fluid on the evolution of the diamond-forming system varies. Its $CO_2$ component initiates the carbonatization of silicate components in the diamond-forming system, increasing the mass of the carbonate constituents. Therewith, the $H_2O$ component, comprising ~50% of the C-O-H-fluid, completely dissolves in the silicate-carbonate melt and, together with the carbonate constituents, essentially lowers

the temperature of the olivine peritectic reaction to 1000–1020 °C in the diamond-forming system solidus.

The release of supercritical $H_2O$ fluid from the melt as a result of the crystallization of the solidus melt results in its existence under subsolidus conditions and correspondingly in the splitting of the subsolidus substance into diamond-bearing magmatic and hydrothermal systems which interact with one another in open conditions.

## References

1. Sobolev, N.V. *Deep-Seater Inclusions in Kimberlites and the Problem of the Composition of the Upper Mantle*; American Geophysical Union: Washington, DC, USA, 1977; 259p. [CrossRef]
2. Litvin, Y.A.; Kuzyura, A.V.; Bovkun, A.V.; Varlamov, D.A.; Limanov, E.V.; Garanin, V.K. Genesis of diamondiferous rocks from upper-mantle xenoliths in kimberlite. *Geochem. Int.* **2019**, *58*, 243–270.
3. Dawson, J.B. Basutoland kimberlites. *Bull. Geol. Soc. Am.* **1962**, *73*, 545–560.
4. Kushiro, I.; Aoki, K. Origin of some eclogite inclusions in kimberlite. *Am. Min.* **1968**, *53*, 1347–1367.
5. MacGregor, I.D.; Carter, J.L. The chemistry of clinopyroxenes and garnets of eclogite and peridotite xenoliths from the Roberts Victor Mine, South Africa. *Phys. Earth Planet. Inter.* **1970**, *3*, 391–397.
6. Prinz, M.; Manson, D.V.; Hlava, P.F.; Keil, K. Incluions in diamonds: Garnet lherzolite and elogite assemblages. *Phys. Chem. Earth* **1975**, *9*, 797–816.
7. Litvin, Y.A. *Genesis of Diamonds and Associated Phases*; Springer Mineralogy: Berlin/Heidelberg, Germany, 2017; 137p. [CrossRef]
8. Sobolev, N.V. Eclogites and pyrope peridotites from the kimberlites of Yakutia. *Phys. Earth Planet. Inter.* **1970**, *3*, 398–404.
9. Ringwood, A.E. *Composition and Petrology of the Earth's Mantle*; McGraw-Hill: New York, NY, USA, 1975; 618p.
10. O'Hara, M.J.; Yoder, H.S. Formation and fractionation of basic magmas at high pressures. *Scott. J. Geol.* **1967**, *3*, 67–117.
11. O'Hara, M.J. The bearing of phase equilibria studies in synthetic and natural systems on the oigin and evolution of basic and ultrabasic rocks. *Earth-Sci. Rev.* **1968**, *4*, 69–133.
12. O'Hara, M.J.; Saunders, M.; Mercy, E.L.P. Garnet peridotite, possible ultrabasic magmas and eclogite interpretation of upper mantle processes in kimberlite. *Phys. Chem. Earth* **1975**, *9*, 681–713.
13. Dawson, J.B. *Kimberlites and Their Xenoliths*; Springer: Berlin/Heidelberg, Germany; New York, NY, USA, 1975; 252p.
14. Yoder, H.S. *Generation of Basaltic Magma*; National Academy of Sciences: Washington, DC, USA, 1976; 265p.
15. Litvin, Y.A.; Spivak, A.V.; Kuzyura, A.V. Fundamentals of the Mantle Carbonatite Concept of Diamond Genesis. *Geochem. Int.* **2016**, *54*, 839–857.
16. Litvin, Y.A. *Physicochemical Studies of Melting of Materials from the Deep Earth*; Nauka: Moscow, Russia, 1991; 312p.
17. Kushiro, I. The system diopside-forsterite-enstatite at 20 kilobars. *Carnegie Inst. Wash. Year B.* **1964**, *63*, 101–108.
18. Davis, B.T.C. The system enstatite-diopside at 30 kilobars pressure. *Carnegie Inst. Wash. Year B.* **1963**, *62*, 103–107.
19. Gasparik, T.; Litvin, Y.A. Stability of $Na_2Mg_2Si_2O_7$ and melting relations on the forsterite-jadeite join at pressures up to 22 GPa. *Eur. J. Mineral.* **1997**, *9*, 311–326.
20. Litvin, Y.A.; Kuzyura, A.V.; Limanov, E.V. The role of garnetization of olivine in the olivine-diopside-jadeite system in the ultramafic-mafic evolution of upper-mantle magmatism (experiment at 6 GPa). *Geochem. Int.* **2019**, *57*, 1045–1063.
21. Marakushev, A.A. Peridotite nodules in kimberlites as indicators of deep lithosphere structure. In *Reports of Soviet Geologists at the 27th International Session of the International Geological Congress*; Petrology: Moscow, Russia, 1984; pp. 153–160.
22. Litvin, Y.A.; Kuzyura, A.V. Peritectic reaction of olivine in the olivine-jadeite-diopside-garnet-(C-O-H) system at 6 GPa as the key mechanism of the magmatic evolution in the upper mantle. *Geochim. Int.* **2021**, *59*, 813–839.
23. Harte, B. Diamond formation in the deep mantle. The record of mineral inclusions and their distribution in relation to mantle dehydration zone. *Mineral. Mag.* **2010**, *74*, 189–215.

24. Andersen, T.; Neumann, F.R. Fluid inclusions in mantle xenoliths. *Lithos* **2001**, *55*, 301–320.
25. Abramson, E.H.; Bollengier, O.; Brown, J.M. The water-carbon dioxide miscibility surface to 450°C and 7 GPa. *Am. J. Sci.* **2017**, *317*, 967–989.
26. Wang, H.; Zeuschner, J.; Eremets, M.; Troyan, I.; Willams, J. Stable solid and aqueous $H_2CO_3$ from $CO_2$ and $H_2O$ at high pressure and high temperature. *Sci. Rep.* **2016**, *6*, 19902. [CrossRef]
27. Rhines, F.N. *Phase Diagrams in Metallurgy: Their Developments and Application*; McGraw-Hill Book Company: New York, NY, USA; Toronto, ON, Canada; London, UK, 1956; 348p.
28. Palatnik, L.S.; Landau, A.I. *Phase Equilibria in Multicomponent Systems*; Holt, Rimehart and Winston Inc.: New York, NY, USA, 1967.
29. Koziol, A.M.; Newton, R.C. Experimental determination of the reaction magnesite + enstatite = forsterite + $CO_2$ in the range 6–25 kbar and 700–1100 °C. *Am. Miner.* **1998**, *83*, 213–219.
30. Litvin, Y.A. High-pressure mineralogy of diamond genesis. In *High-Pressure Mineralogy*; Ohtani, E., Ed.; Geological Society of America: Boulder, CO, USA, 2007; Volume 421, pp. 83–103.
31. Vinogradov, A.P.; Kropotova, O.I.; Ustinov, V.I. Possible carbon sources for natural diamonds according to isotopic data. *Geochemistry* **1965**, *6*, 543–552.
32. Galimov, E.M. *Geochemistry of Stable Isotopes of Carbon*; Nedra: Moscow, Russia, 1968; 266p.
33. Javoy, M.; Pineau, F.; Delorme, H. Carbon and nitrogen in the mantle. *Chem. Geol.* **1986**, *57*, 41–62.